In vivo acquisition of CEST MRI using Length and Offset VARiation of Saturation CEST (LOVARS-CEST) for artifact reduction

X. Song[1,2], G. Liu[1,3], A. Bar-Shir[1,2], M. Gorelik[1,2], A. A. Gilad[1,2], P. C. Van Zijl[1,3], J. W. Bulte[1,2], and M. T. McMahon[1,3]

[1]Division of MR Research, The Russell H. Morgan Department of Radiology and Radiological Science, The Johns Hopkins University, Baltimore, MD, United States, [2]Cellular Imaging Section, Institute for Cell Engineering, Johns Hopkins University, Baltimore, MD, United States, [3]F.M. Kirby Research Center, Kennedy Krieger Institute, Baltimore, MD, United States

Introduction MRI is well established as a means for characterizing brain tumors. Chemical Exchange Saturation Transfer (CEST) MRI[1] has been shown to allow the detection of high-grade gliomas[2] without use of gadolinium, the contrast agents that may pose risks for patients with renal insufficiency. Most existing CEST schemes rely on acquiring many saturation frequency offsets to correct for B_0 inhomogeneities, which is time-consuming and inefficient[3,4]. One alternative is to use WALTZ-16 pulse trains for On-Resonance saturation[5,6], but specificity is lost for this approach. Here we propose a new method termed "Length and Offset VARiation of Saturation" (LOVARS) CEST, which utilizes saturation length variations to modulate CEST, magnetization transfer (MT) and direct water saturation (DS) contrasts in a manner to provide B0 correction, also allowing CEST post-processing techniques similar to those used to analyze event-related fMRI. The resulting modulations can be separated using a number of transformations, and we have tested using Fourier analysis to separate CEST from the other components using LOVARS data acquired on mice bearing 9L brain tumors, a tumor model well studied previously for CEST imaging due to the increased content of cellular proteins and peptides.

Methods and Materials 8 Balb/c NOD SCID male mice (6-8 weeks) were inoculated with $2x10^5$ 9L gliosarcoma cells at 2 mm right of bregma and 2.5 mm ventral position within the brain. Images were acquired on a Bruker 9.4T horizontal bore animal MR system with a 25mm-diameter sawtooth transmit/receive coil from Day4 to Day11 after transplantation. The mice were anesthetized with 0.5-2% isoflurane to keep the respiratory rate at 30-50/minute. The LOVARS scheme consists of N (N=3 or 4) LOVARS Units (LUs) with four saturation images per LU, [(-Δω, T_{sat}#2), (-Δω, T_{sat}#1), (+Δω, T_{sat}#2), (+Δω, T_{sat}#1)]$_n$, where n=0,1,…,N, Δω is the frequency of the saturation pulse with respect to water, and T_{sat}#1, T_{sat}#2 are the two different saturation pulse lengths with T_{sat}#2 < T_{sat}#1. One coronal slice (1mm thick) at the center of the tumor was chosen with parameters: matrix size 128x64, FOV 1.65x1.5cm, TR/TE=5000ms/14.59ms, RARE Factor 8, NA=2; T_{sat}#1=3s, T_{sat}#2=0.8s, B1=3μT, Δω=+/-3.5ppm. The modulation patterns produced by this saturation variation were analyzed on a pixel-by-pixel basis through Fourier Transformation of the 12-16 images from LOVARS time domain (LU) to LOVARS frequency domain (cycles/LU). All image analysis was performed using Matlab.

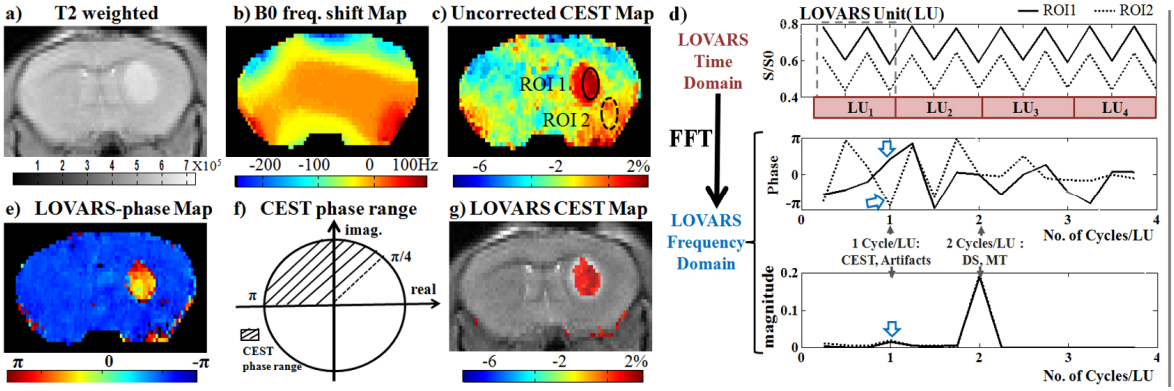

Fig. 1 LOVARS contrast maps 8 days after transplantation to demonstrate the principle of LOVARS-CEST

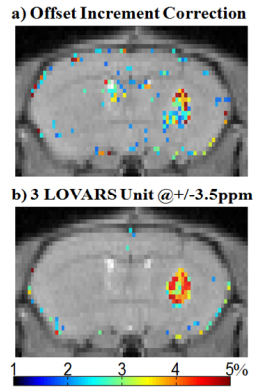

Fig.2 Images Comparison

Results and Discussion The LOVARS method is designed to modulate contrast that are symmetrical with respect to water (MT and DS) at an oscillation rate twice as fast as asymmetric contrast (CEST and B0 perturbations of water and MT) and to distinguish contrast that builds up fast (MT, DS) from slow (CEST). We acquired 17 different LOVARS-CEST images on mice bearing 9 L gliosarcomas between 4 and 11 days after transplantation. Fig.1 shows representative MR images acquired on a mouse 8 days after transplantation with Fig.1a) showing a T2w image. Fig.1b) is the WASSR B0 map for the brain displaying field inhomogeneities which distort the CEST image (Fig.1c)). The CEST image was generated using two images with saturation offsets of +/-3.5ppm to calculate MTRasym, which results in artifacts in the lower right hemisphere where there is normal brain tissue but (from the B0 map) water is shifted +80Hz. Fig.1d) shows the LOVARS signal patterns for two ROI's drawn in Fig.1c) both before and after FFT. We performed an FFT on a pixel-by-pixel basis on the signal patterns and examine the resulting magnitude and phase at a LOVARS frequency of 1cycle/LU (marked by blue arrows in Fig1d). The imaginary component corresponds to MTR_{asym} (T_{sat}#1), the real component is MTR_{asym}(T_{sat}#2), and the phase between these components (φ) is given by: tan(φ) = MTR_{asym} (T_{sat}#1)/ MTR_{asym} (T_{sat}#2), representing a buildup map for saturation contrast. The LOVARS-phase map (Fig.1(e)) displays better separation of CEST contrast regions than the uncorrected MTR_{asym} map (Fig. 1c), with the CNR between tumor and normal brain tissue ~10 fold higher for 12/17 experiments which possessed B0 shifts varying by 150Hz or less. Moreover, as MTR_{asym} (T_{sat}#1) > MTR_{asym} (T_{sat}#2) for CEST contrast, φ should be between π/4 and π for *in vivo* imaging (Fig.1f). This LOVARS phase map can be used to mask the uncorrected CEST images, leading to a LOVARS contrast map in Fig. 1g only showing the MTR_{asym} contrast within the tumor. Compared with the offset correction method[3-5](Fig.2a, obtained using 3 sat. freqs. which are separated by 100Hz and placed on both sides of water), LOVARS generates cleaner contrast maps with higher CNR for a similar acquisition time(Fig.2b) when the B0 shifts vary by 250Hz or less, potentially allowing the detection of smaller or more infiltrative tumor.

Conclusion LOVARS-CEST can be used to remove B0 inhomogeneity artifacts and increase the CNR for CEST imaging of brain tumors *in vivo*.

Reference: 1. Hancu, et al., Acta Radiol. 2010, 51:910-23. 2. Wen, et al., Neuroimage, 2010, 51:616-22. 3. Stancanello, et al., CMMI, 2008, 3:136-149. 4. Kim, et al., MRM, 2009, **61**:1441-1450. 5. Li, et al., Magn Reson Med. 2009, 62:1282-916. 6. Vinogradov, et al., JMR, 2005, 176:54-63.